



Data acquisition with real-time numerical integration for COMPASS-U magnetic diagnostics

A. Torres^{a,b,*}, B.B. Carvalho^b, T. Markovic^{a,c}, A.J.N. Batista^b, A. Havranek^a, V. Weinzettl^a, H. Fernandes^b

^a Institute of Plasma Physics of the CAS, Za Slovankou 1782/3, Prague 8, 182 00, Czech Republic

^b Instituto de Plasmas e Fusão Nuclear, Instituto Superior Técnico, Av. Rovisco Pais 1, Lisbon, 1049-001, Portugal

^c Charles University, Faculty of Mathematics and Physics, Ke Karlovu 3, Prague 2, 121 16, Czech Republic

ARTICLE INFO

Keywords:

Magnetic diagnostic
Magnetics
Data acquisition
Real-time
Tokamak
ATCA

ABSTRACT

The COMPASS-U tokamak will feature a completely new set of magnetic diagnostics from sensors to data acquisition. In order to control and reconstruct the plasma magnetic equilibrium, the inductive magnetic sensor signals are integrated and processed. For this purpose, a modular data acquisition solution with digital integration is proposed for COMPASS-U. Based on the ATCA platform, and continuing the development path of the low-drift integrators for W7-X and ITER, this solution allows a high degree of flexibility and scalability with state-of-the-art performance that can benefit a machine with different operational stages and scientific goals over years of operation. This article details the effort to qualify the data acquisition electronics on COMPASS, how to take advantage of real-time processing to enhance the dynamic range through composition of signals sampled with different input ranges and bandwidth, and the implementation of a strategy to mitigate the loss of signal integrity when using such a composition of signals.

Tests on COMPASS showed that the digital integration performs well with real probe signals for basic control purposes even in the presence of fast events. A real-time compatible algorithm to recover high-frequency components was also successfully tested, albeit with significant noise added, while simulation shows that obtaining a signal from two different sampling sources can increase the dynamic range with minimal impact on the signal integrity.

1. COMPASS-U and magnetic diagnostics

COMPASS-U is a medium sized, high magnetic field tokamak being projected at IPP Prague ($R = 0.894$ m, $a = 0.27$ m, $B_1 = 5$ T, $I_p = 2$ MA) [1,2]. One of the distinguishing features of this device is the full recycling regime, enabled by the operation at high temperatures (up to 500 °C) of the fully metallic first wall and vacuum vessel. This feature leads to several challenges in diagnostics development [3], and in particular, to the magnetic diagnostic [4,5].

Inductive magnetic sensors provide important insight into localized and global plasma parameters such as current and energy, as well as the magnetic field distribution and strength, inside and outside the vacuum vessel, which in turn is used to reconstruct the plasma equilibrium and control its position in the vessel. In order to achieve this, the voltage at the end of the coils and loops most times need to be integrated to obtain quantities proportional to the magnetic fields or currents. In doing so, any small DC offset that is integrated with the signal, has the potential to generate a large linear drift on the integrated data. This is

of particular concern for real-time needs. Regardless of whether analog or numerical, the integration electronics should be calibrated before measurement and introduce as little offset as possible.

New or upgraded devices often put a considerable research effort in minimizing integration drift with either new techniques or taking advantage of the continuous performance improvements in the field of electronics. For devices with long pulse durations this is a key focus and great efforts are being made to minimize integration drift [6–9]. However, even for machines with shorter pulses where the error does not have as much time to accumulate, it can still amount to a significant degradation of some of the most useful signals for engineering and physics exploitation.

On COMPASS-U, new integrators have to be developed as the ones used in COMPASS are insufficient in both number or performance. A particularly attractive design is the digital integration with pulse switched modulation described in [10] used at ISTTOK [11] and W7-X [12], due to no need for independent integration circuits (combines

* Corresponding author at: Institute of Plasma Physics of the CAS, Za Slovankou 1782/3, Prague 8, 182 00, Czech Republic.

E-mail address: torres@ipp.cas.cz (A. Torres).

#18391 Mirnov C3

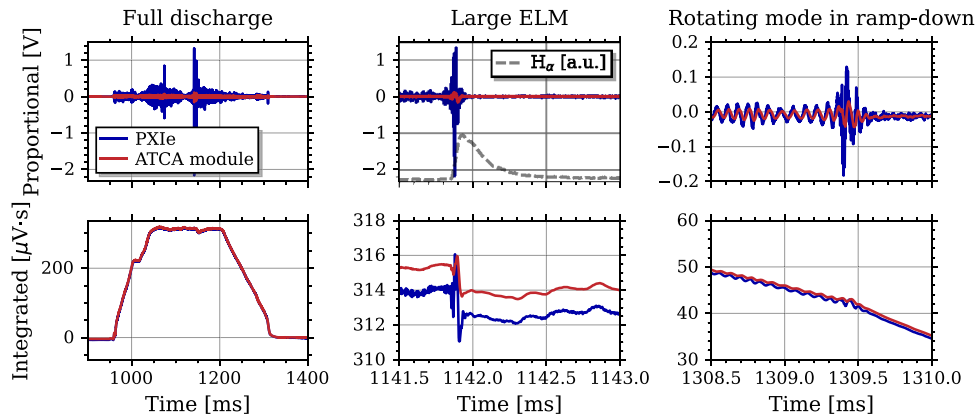


Fig. 1. Proportional (sampled, top) and integrated (bottom) signals of a Mirnov coil for the ATCA modules (real-time integration with pre-discharge calibration) and NI PXIe (offline digital integration and drift compensation) for a COMPASS discharge. First column shows the full discharge, middle shows a ms scale detail of a strong ELM (H_{α} signal shown for reference) and on the last column, detail of a rotating island observed on the ramp-down. While an order of magnitude reduction of the non-integrated signal amplitude is visible for fast events, the integral is largely unaffected, even on a sub-millisecond scale.

integration with data acquisition) and its implementation in both the Advanced Telecommunications Computing Architecture (ATCA) hardware and MARTE real-time control software, both used previously on COMPASS.

2. Qualification of the real-time digital integration on COMPASS tokamak

While the COMPASS tokamak was still in operation [13], the digital integration system was tested on Mirnov coil signals. The testing of this system was made easier as COMPASS made use of several ATCA MIMO-ISOL data acquisition boards [14,15]. Using this existing hardware, it was simple to implement the Data Acquisition (DAQ) modules and firmware used on ISTOK and W7-X. In both these devices the ATCA MIMO-ISOL data acquisition boards, featuring a XILINX Virtex-4 FPGA, perform the digital integration with pulse switched modulation in real-time control cycles of 50 μ s, the maximum control frequency to be used on COMPASS-U.

Two in-vessel Mirnov coils (poloidal field, array C) [16] sampled simultaneously by a National Instruments PXIe-6368 16 bit DAQ board, and the ATCA 18 bit integration modules. Both systems have 2 MSPS sampling rate. The firmware was configured to output through Direct Memory Access (DMA) full non-integrated data, the integral computed in real-time, as well as the chopper status. Data was collected during one experimental day, with calibration of the offsets being carried out in operational breaks between pulses. The procedure for calibration is described in [12] and requires the measurement of an Electrical Offset (EO) that does not change substantially over time and a Wiring Offset (WO) that can change with environmental conditions. The offset values are transferred to the FPGA that corrects subsequent discharges in real-time.

The signal time evolution in Fig. 1 shows the comparison of the signal sampled by both DAQ and their integration for different timescales. The integrator electronics features an input filter, implemented as a first order RC low-pass filter with cutoff frequency of 8.813 kHz. Its attenuation is particularly noticeable on the proportional signal. The configurable chopping frequency was set to 1 kHz for all discharges.

The basic control systems (current, vertical position, etc.) relies only on slow signals (below 1 kHz), therefore the loss of detail observed on the integrated data is not very relevant, as the controller cannot react to fast perturbations on this timescale. Introduced delay is only visible at the μ s scale. Likewise in the ramp-up and ramp-down, no degradation that can be attributed to the filter is observed.

Instabilities and magnetohydrodynamic (MHD) activity will introduce large voltages due to the very high dB/dt in comparison to the equilibrium signal. The integrated signal integrity is retained despite high reduction of the sampled signal. The fine (high frequency) detail filtered is in itself sometimes a positive feature, as high, fast transitions could trigger unwarranted responses by real-time controllers.

Since there is no analogue integrator reference signal for comparison, it is difficult to quantify to what extent the MHD activity might have influenced the integration. However, across all acquired discharges, no significant loss of integrated signal was observed, with the integrated signals returning to the zero reference before the discharge. Likewise, the chopper transitions did not compromise the signal integrity to any level noticeable in time or frequency domain. The small linear drift observed is negligible on ~ 1 s long discharges of COMPASS.

2.1. Recovery of high-frequency components from filtered data

In the early stages of ITER conceptual design, an experimental hybrid analogue–digital integrator was proposed [17] with a similar input filter. The key concept was to take advantage of the fact that the filter is already integrating the signal beyond its cutoff frequency (f_c), with only the slow part of the signal needing additional integration. The reconstructed integral of the input voltage (V_0) has an integral and proportional dependence on the voltage after the filter (V_1 , sampled as V_i):

$$\int V_0 dt = \int V_1 dt + RC V_1 \approx \sum V_i \Delta t + RC V_i. \quad (1)$$

Fig. 2 shows the amplitude and phase transfer functions of the ideal integrator, the input filter, and the high frequency recovery process, providing a visual interpretation of the technique in the frequency domain. Moreover, this digital reconstruction only requires the current sample, and is therefore real-time compatible.

The first order filter at the input stage of the ATCA DAQ module mostly serves the purpose of reducing the dynamic range of the signal to be sampled, leaving the bandwidth of interest unaltered. However, having recorded all data at the sampling rate, and having knowledge of the low-pass filter cutoff frequency used ($f_c = 8.813$ kHz), it is possible to evaluate the high frequency recovery technique.

Fig. 3 shows that the details of the high-frequency events (consequently where the impact of the filter is larger) were successfully recovered at the sub-millisecond scale.

On the frequency domain – Fig. 4 – a more comprehensive picture can be drawn. Firstly, ATCA module spectrogram reinforces the observation in Fig. 1 that the major MHD activity features are still observed,

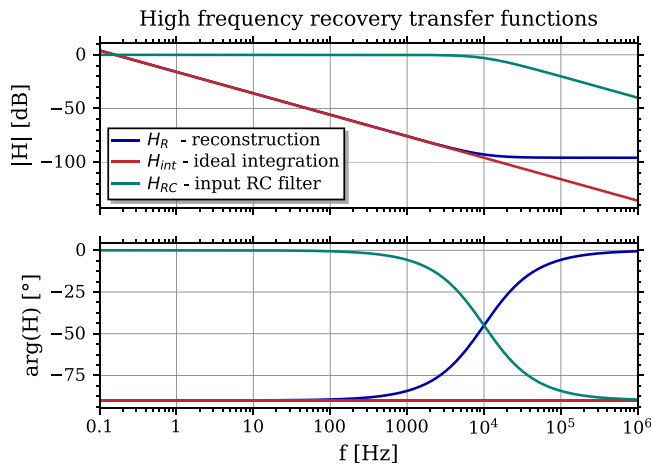


Fig. 2. Amplitude and phase transfer functions for the ideal integration, a first order low-pass filter ($f_c = 10$ kHz) and the reconstruction technique. When combined, these two processes recover the ideal integration (red curve).

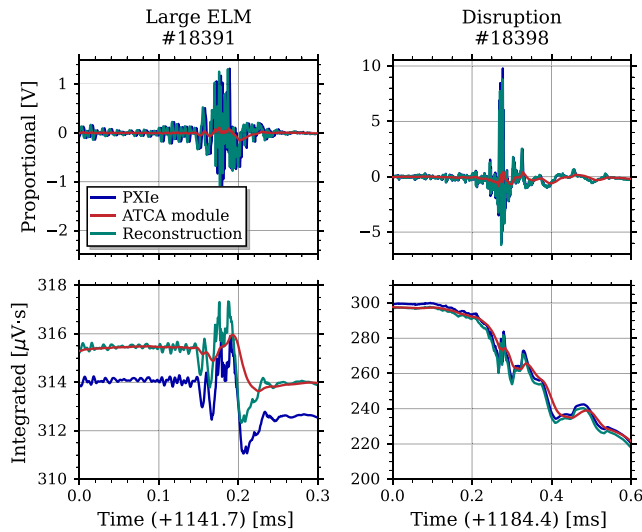


Fig. 3. Demonstration of the high frequencies' reconstruction technique in time domain for two features with high frequency components: on the left a large ELM and on the right a disruption. Plots on the top show the coil voltage and on the bottom the corresponding integrated signal. Blue line shows the reference signal, while the green is reconstructed from the analogue filtered ATCA signal (red trace).

either by manifesting themselves in the unattenuated bandwidth or by the strength of its signal, well above the equilibrium components. On the reconstruction spectrogram two main conclusions can be drawn: (i) the filtered components were recovered to a point that it does not hinder physics analysis in frequency domain; (ii) there is a considerable addition of noise, visible on the vacuum signal before and after the plasma discharge.

The source of this noise is in the electronic circuits, amplified by the reconstruction technique. The noise is not subject to the input filter attenuation, but is subject to the digital reconstruction, nonetheless. This results in a net amplification as can be seen in the transfer functions in Fig. 2.

Due to the added noise, and since real-time applications do not require the measurement of high frequency signals, this reconstruction technique will not be implemented in real-time for COMPASS-U. Notwithstanding, it will be possible to implement the technique offline since the non-integrated data will be saved and streamed post-discharge.

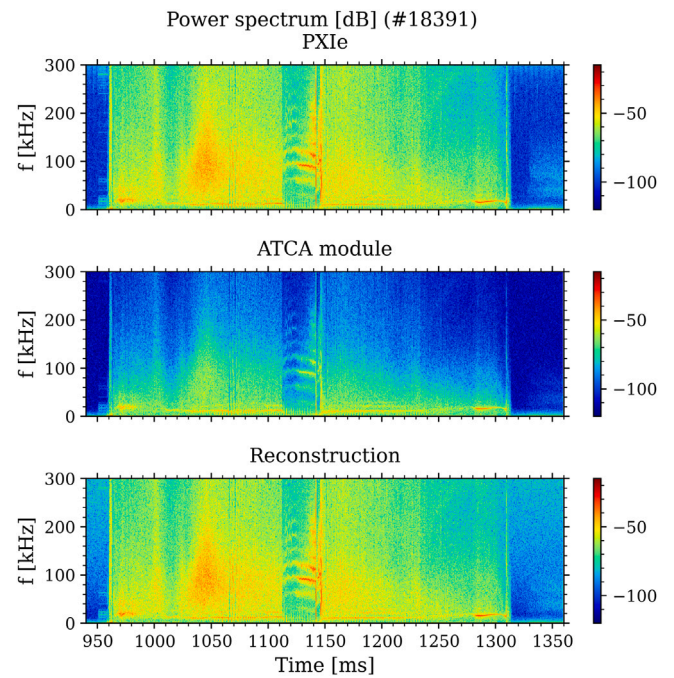


Fig. 4. Power spectrograms for the reference 16 bit DAQ signal (top), the ATCA module, where the analogue filtering is noticeable (middle) and the result of the reconstruction technique (bottom). The reconstructed signal is indistinguishable from the reference one while there is plasma. However, on the vacuum part, before and after, significant noise is observed.

High frequency oscillations will be acquired by a different set of coils [5], sampled without filtering. If these cannot be used due to a high number of failures or complete inoperability during campaigns at elevated temperatures (500 °C), the technique is a useful backup solution. It was shown that MHD activity can be recovered from the more reliable coils, connected to the real-time digital integrators, as in Fig. 4.

3. Two-channel modular solution for COMPASS-U

With the solution tested on COMPASS, a concept is proposed for COMPASS-U, with new, procurable electronic components but based on a previously developed system [18]. The key difference to the tested modular system is the architecture of two channels per module.

On COMPASS and other tokamaks it is common practice to sample some magnetic sensors with two DAQ channels, either high/low input range, due to the high dynamic range of the signals or integrated/non-integrated. A two channel solution would allow this split to be performed to any or all signals without additional hardware or cable splits. On the other hand, if two channels are not needed, the system can be used for different sensors, reaching a high channel density. By developing the system from the start with a high level of flexibility in mind and having control over the hardware development, the system can be adapted to a staged operation (at very different plasma scenarios) and consequently also staged deployment of magnetic diagnostics at minimal hardware changes and cost.

The two channel configuration is envisioned to have three operation modes:

- Individual sampling with one coil per channel with a given bandwidth and input range, achieving the highest channel density.
- Parallel sampling, whereby a single sensor is sampled with two different bandwidths and input ranges. Two real-time data-streams per sensor.

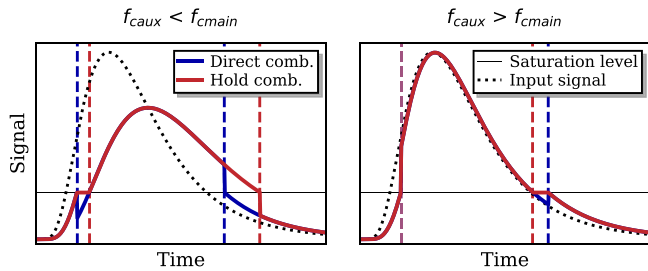


Fig. 5. Illustration of the two channel composition methods. On the left-hand side the case where the cutoff frequency of the auxiliary channel is larger than that of the main channel while on the graph on the right-hand side shows the opposite scenario. The voltage corresponding to the ADC saturation of the main channel is represented by the horizontal black line. The vertical dashed lines indicate the moments of the switch between channels, for each method. The ‘hold’ combination holds the active channel until both channels cross the threshold voltage corresponding to the saturation of the ADC on the main channel.

- Extended dynamic range sampling, using an auxiliary high input range channel to recover the integral lost due to the saturation of the main high-resolution channel. One real-time data stream per sensor.

The decision of which operation mode for each sensor can be made by the user at the FPGA firmware level for each board with 24 modules. With multiple boards being considered, this will allow using two channels only for selected high-priority sensors and only one channel for the remaining sensors.

Modules with this configuration were designed with up-to-date components and prototypes are currently being tested. Description and results of the prototypes are to be presented in a future paper.

3.1. Extended dynamic range implementation

Merging data from two different sources in real-time may lead to substantial errors. This process is only advantageous if the error is smaller than that caused by the saturation. In this particular case, the high sampling rate in conjunction with the analogue filter mitigate the loss of signal due to fast transients. Knowing that for magnetic signals, saturation would occur during disruptions or fast MHD events, possibly in close proximity of the sensor, we can expect high voltage peaks, spanning in the μs range.

Considering that both channels have different bandwidths, defined by an input filter at different cutoff frequencies, two strategies can be employed, triggered by ADC saturation of the main channel: (i) direct — direct transition from the main to the auxiliary channel upon (de)saturation of the first ADC; (ii) hold — transition to and from the auxiliary channel when both reach the voltage threshold for the saturation of the ADC on the main channel. By directly switching between the channels upon ADC saturation, the differential time delay introduced by the filters is neglected. The ‘hold’ method tries to compensate for the lag between the two channels on the rising and falling edges of the pulse by holding the currently active channel, in effect ‘waiting’ for the slower response of the other channel. Fig. 5 provides a graphical illustration of the two combination methods on a generic pulse.

In order to evaluate the theoretical performance of both methods, data from COMPASS Mirnov coil and flux loop sampled at 2 MSPS was re-sampled via a synthetic diagnostic, simulating the input filter with attenuator (resistor divider), the ADC and the merging algorithm. The error introduced was then evaluated and shown in Fig. 6 for a Mirnov coil signal, with an artificial saturation at a given threshold introduced. The simulation shows that (i) for small differences between the cutoff frequencies of the filters, both methods result in minimal error; (ii) the hold strategy only outperforms the simple composition if auxiliary channel has a lower cutoff than the main channel, that is,

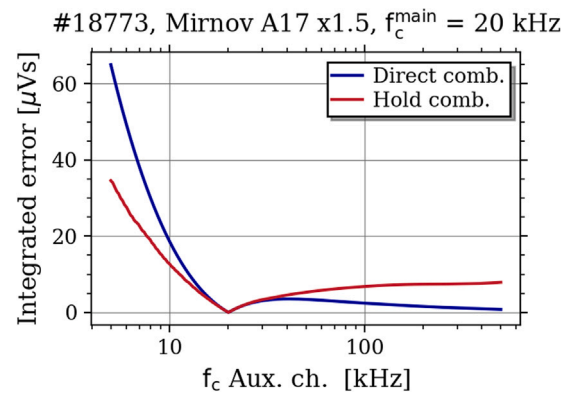


Fig. 6. Simulation of error in integrated data added due to the combination of synthetic diagnostic channels of the same signal with different input ranges (5 V, 100 V) as function of the cutoff frequency of the auxiliary channel, having the main channel $f_c = 20$ kHz. It is noticeable that the hold combination minimizes the error if the auxiliary channel has a lower bandwidth. If the filters of both channels have similar f_c , both methods perform identically.

when the auxiliary channel lags behind the main; (iii) in either case, a smaller error is introduced with a higher bandwidth on the auxiliary channel. These conclusions are similar for different magnetic sensors, with changes to the absolute magnitude of the error introduced, which in general is much smaller than that observed when integrating a saturated signal. It will always be preferred to have similar bandwidth on both channels, but errors of few $\mu\text{V s}$ are small even for the sensors of lowest signal.

4. Conclusions

The digital integration with modulation technique was studied at COMPASS-U with good results. Beyond having negligible linear drift for COMPASS-U pulse lengths (≤ 10 s), the high dynamic range, characteristic of magnetic signals with MHD activity did not impact the signal integrity on position control and equilibrium reconstruction timescales. Still, in order to prevent unnecessary delay introduced on the control loop when responding to fast plasma movements, a higher bandwidth is considered for COMPASS-U modules. It was also shown how the detail on fast events can be recovered, in real-time or post-processing, albeit with a trade-off in added noise. COMPASS-U will have dedicated probes with no integration envisioned for detection and study of fast events. However, this technique will be considered in case operation must rely fully on the coils sampled by the integration modules.

The new modules for COMPASS-U will feature two channels, which will bring added flexibility to the operation. In the case where the dynamic range of a magnetic probe or flux loop requires different input ranges and bandwidths, merging these two sources was shown to be possible with minimal error introduced.

The signal processing described adds only a small number of operations that, when implemented in a modern FPGA, amount to a negligible overhead. The real-time performance of the implementation will be evaluated in a new ATCA carrier board featuring a XILINX Zynq Ultrascale+ FPGA to be reviewed in a dedicated article.

Declaration of competing interest

The authors declare that they have no known competing financial interests or personal relationships that could have appeared to influence the work reported in this paper.

Data availability

Data will be made available on request.

Acknowledgements

This work has been carried out within the framework of the EUROfusion Consortium, funded by the European Union via the Euratom Research and Training Programme (Grant Agreement No 101052200 – EUROfusion); and of the project COMPASS-U: Tokamak for cutting-edge fusion research (No. CZ.02.1.01/0.0/0.0/16_019/0000768) and co-funded from European structural and investment funds and by MEYS project LM2018117. Views and opinions expressed are however those of the author(s) only and do not necessarily reflect those of the European Union or the European Commission. Neither the European Union nor the European Commission can be held responsible for them. A. Torres was supported by the Fundação para a Ciência e Tecnologia through the Instituto de Plasmas e Fusão Nuclear, a research institute of Instituto Superior Técnico, under the Ph.D. grant PD/BD/142968/2018.

References

- [1] R. Panek, et al., Conceptual design of the COMPASS upgrade tokamak, *Fusion Eng. Des.* 123 (2017) 11–16, <http://dx.doi.org/10.1016/j.fusengdes.2017.03.002>, Proceedings of the 29th Symposium on Fusion Technology (SOFT-29) Prague, Czech Republic, September 5-9, 2016.
- [2] P. Vondracek, R. Panek, M. Hron, J. Havlicek, V. Weinzettl, T. Todd, D. Tskhakaya, G. Cunningham, P. Háček, J. Hromadka, P. Junek, J. Krbec, N. Patel, D. Šesták, J. Varju, J. Adamek, M. Balazsova, V. Balner, P. Barton, H. Zhang, Preliminary design of the COMPASS upgrade tokamak, *Fusion Eng. Des.* 169 (2021) 112490, <http://dx.doi.org/10.1016/j.fusengdes.2021.112490>.
- [3] V. Weinzettl, J. Adamek, P. Bilkova, J. Havlicek, R. Panek, M. Hron, O. Bogar, P. Bohm, A. Casolari, J. Cavalier, R. Dejarnac, M. Dimitrova, I. Duran, S. Entler, O. Ficker, P. Háček, J. Horacek, M. Imrisek, F. Jaulmes, J. Zajac, Constraints on conceptual design of diagnostics for the high magnetic field COMPASS-U tokamak with hot walls, *Fusion Eng. Des.* 146 (2019) <http://dx.doi.org/10.1016/j.fusengdes.2019.03.020>.
- [4] A. Torres, K. Kovarik, T. Markovic, J. Adamek, V. Weinzettl, B. Carvalho, H. Fernandes, M. Hron, R. Panek, Mineral insulated cable assessment for inductive magnetic diagnostic sensors of a hot-wall tokamak, *J. Instrum.* 14 (09) (2019) C09043, <http://dx.doi.org/10.1088/1748-0221/14/09/c09043>.
- [5] A. Torres, K. Kovarik, T. Markovic, J. Adamek, I. Duran, R. Ellis, M. Jerab, J. Reboun, P. Turjanica, V. Weinzettl, H. Fernandes, Test bench for calibration of magnetic field sensor prototypes for COMPASS-U tokamak, *Fusion Eng. Des.* 168 (2021) 112467, <http://dx.doi.org/10.1016/j.fusengdes.2021.112467>.
- [6] Y. Wang, Z.S. Ji, Z.C. Zhang, S. Li, F. Wang, X.Y. Sun, Upgrade of the analog integrator for EAST device, 2018, <http://dx.doi.org/10.48550/ARXIV.1806.08530>.
- [7] Y. Xu, X. Ji, Q. Yang, T. Sun, B. Yuan, S. Liang, L. Ren, J. Zhou, Development of a low-drift integrator system on the HL-2A tokamak, *Rev. Sci. Instrum.* 87 (2016) 023507, <http://dx.doi.org/10.1063/1.4940027>.
- [8] J.G. Bak, S.G. Lee, D. Son, E.M. Ga, Analog integrator for the Korea superconducting tokamak advanced research magnetic diagnostics, *Rev. Sci. Instrum.* 78 (2007) 043504, <http://dx.doi.org/10.1063/1.2721405>.
- [9] A.J. Batista, L. Capella, A. Neto, S. Hall, G. Naylor, A. Stephen, J. Sousa, B. Carvalho, F. Sartori, R. Campagnolo, I. Bas, B. Goncalves, S. Arshad, G. Vayakis, S. Simrock, L. Zabeo, F4E prototype of a chopper digital integrator for the ITER magnetics, *Fusion Eng. Des.* 123 (2017) 1025–1028, <http://dx.doi.org/10.1016/j.fusengdes.2017.02.024>, Proceedings of the 29th Symposium on Fusion Technology (SOFT-29) Prague, Czech Republic, September 5-9, 2016.
- [10] A. Werner, W7-X magnetic diagnostics: Performance of the digital integrator, *Rev. Sci. Instrum.* 77 (2006) 10E307, <http://dx.doi.org/10.1063/1.2220073>.
- [11] D. Corona, N. Cruz, J.J.E. Herrera, H. Figueiredo, B.B. Carvalho, I.S. Carvalho, H. Alves, H. Fernandes, Design and simulation of ISTTOK real-time magnetic multiple-input multiple-output control, *IEEE Trans. Plasma Sci.* 46 (2018) 2362–2369, <http://dx.doi.org/10.1109/TPS.2018.2815282>.
- [12] B.B. Carvalho, A. Batista, M. Zilker, K. Rahbarnia, A. Werner, C. Team, E. Association, Design, implementation and commissioning of ATCA based high-speed multichannel data acquisition systems for magnetic diagnostics in W7-X, in: 11th IAEA Technical Meeting on Control, Data Acquisition and Remote Participation for Fusion Research, Greifswald, Germany, 2017.
- [13] M. Hron, et al., Overview of the COMPASS results, *Nucl. Fusion* 62 (2022) 042021, <http://dx.doi.org/10.1088/1741-4326/ac301f>.
- [14] D.F. Valcárcel, A. Neto, J. Sousa, B.B. Carvalho, H. Fernandes, J.C. Fortunato, A.S. Gouveia, A.J. Batista, A.G. Fernandes, M. Correia, T. Pereira, I.S. Carvalho, A.S. Duarte, C.A. Varandas, M. Hron, F. Janky, J. Písačka, An ATCA embedded data acquisition and control system for the compass tokamak, *Fusion Eng. Des.* (2009) <http://dx.doi.org/10.1016/j.fusengdes.2008.12.011>.
- [15] D.F. Valcárcel, A. Neto, I.S. Carvalho, B.B. Carvalho, H. Fernandes, J. Sousa, F. Janky, J. Havlicek, R. Beno, J. Horacek, M. Hron, R. Pánek, The COMPASS tokamak plasma control software performance, *IEEE Trans. Nucl. Sci.* (2011) <http://dx.doi.org/10.1109/TNS.2011.2143726>.
- [16] J. Havlicek, O. Kudláček, F. Janky, J. Horáček, R. Beño, D.F. Valcárcel, J. Fixa, J. Brotánková, J. Zajac, M. Hron, R. Pánek, P. Cahyna, Status of magnetic diagnostics on COMPASS, in: WDS'10 Proceedings of Contributed Papers: Part II – Physics of Plasmas and Ionized Media, 2010.
- [17] E.J. Strait, J.D. Broesch, R.T. Snider, M.L. Walker, A hybrid digital–analog long pulse integrator, *Rev. Sci. Instrum.* 68 (1997) 381–384, <http://dx.doi.org/10.1063/1.1147835>.
- [18] B. Gonçalves, J. Sousa, B. Carvalho, A. Batista, A. Neto, B. Santos, A. Duarte, D. Valcarcel, D. Alves, M. Correia, A. Rodrigues, P. Carvalho, J. Fortunato, P. Carvalho, M. Ruiz, J. Vega, R. Castro, J.M. Lopez Navarro, N. Utzel, P. Mota, ITER prototype fast plant system controller based on ATCA platform, 87, 2012, pp. 171–178, <http://dx.doi.org/10.1109/NSSMIC.2011.6154473>,